Chemical Science Review and Letters ISSN 2278-6783

Research Article

Hysteresis, Vibrational Resonance and Chaos in Brusselator Chemical System under the Excitation of Amplitude Modulated Force

S. Guruparan[1], B. Ravindran Durai Nayagam[2], V. Ravichandran[3], V. Chinnathambi[3]* and S. Rajasekar[4]

[1]Department of Chemistry, Sri K.G.S Arts College, Srivaikuntam-628619, Tamilnadu, India
[2]Department of Chemistry, Pope's College, Sawyerpuram-628251, Tamilnadu, India
[3]Department of Physics, Sri K.G.S Arts College, Srivaikuntam-628619, Tamilnadu, India
[4]Department of Physics, Bharathidasan University, Thiruchirapalli-620 024, Tamilnadu, India

Abstract

We consider Brusselator chemical system driven by an amplitude modulated (AM) force. Numerically we study the dynamics of Brusselator chemical system driven by an amplitude modulated force with widely different frequencies ω and Ω (ie. Ω >> ω) and same frequencies (ie. ω = Ω). We show the occurrence of hysteresis and vibrational resonance for the case Ω >> ω and the coexistence of several period-T orbits, bifurcations of them, routes to chaos, quasiperiodic and chaotic orbits for the case ω = Ω. We characterize periodic orbits, quasiperiodic orbits, chaotic orbits, hysteresis and vibrational resonance using bifurcation diagram, maximal Lyapunov exponent, phase portrait, Poincare map and resonance plots.

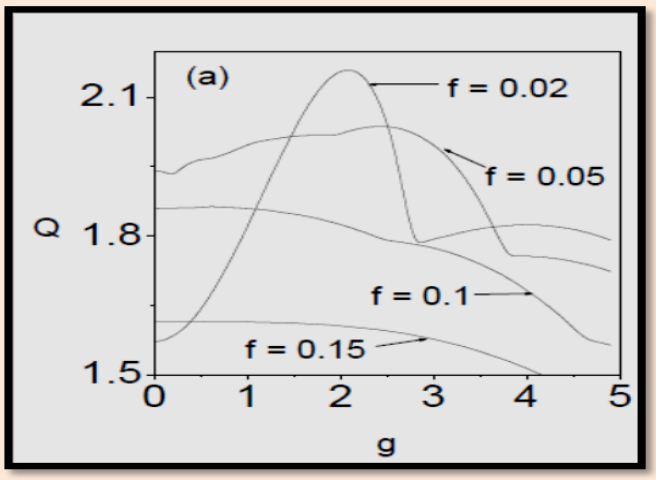

Keywords: Brusselator, Amplitude Modulated Force, Quasiperiodic orbit, Hysteresis, Vibrational Resonance

***Correspondence**
Author: V. Chinnathambi
Emails: vchinna2007@yahoo.in

Introduction

In the past decade the study of complex dynamics and chemistry of oscillating reaction under the influence of external perturbation received much attention and various results such as period doubling bifurcation leading to chaotic motion, quasiperiodic route to chaos, coexistence of multiple attractors, hysteresis, vibrational resonance etc. have been obtained [1-10].

The Brusselator is a theoretical model for a type of autocatalytic reaction. In this type of chemical reaction at least one of the reactants is also a product and the rate of reactions is fundamentally nonlinear. This model was first proposed by Prigogine et al. [11]. It is characterized by the reactions,

$$\begin{aligned} A &\rightarrow X, \\ B + X &\rightarrow Y + D, \\ 2X + Y &\rightarrow 3X, \\ X &\rightarrow E, \end{aligned} \qquad (1)$$

where, the parameters A, B, D and E are constants. The two species X and Y are the autocatalytic species. During the last decade or so remarkable progress has been made in exploring the complexity of Brusselator chemical reaction (Eq.1), where the presence of chaos and other related phenomena have been extensively investigated [12-14]. In an early paper, under the excitation of external periodic force in system (1), Kai et al. [15,16] and Hao and Zhang [17]

have investigated the regular and chaotic response patterns in (f, ω) parameters space. In Refs. [13, 18] the complex dynamical behaviours of the system (1) with periodic and impulsive inputs have been extensively investigated. Recently Ali Sanayei [19] studied the effect of sinusoidal force acted on the Brusselator chemical reaction.

The dynamics of the Brusselator chemical reaction under the excitation of AM force can be described by a system of two first-order differential equations. In dimensional form they are

$$\dot{x} = a - (b + 1)\, x + x^2\, y + (f + 2\, g \cos \Omega t)\, \sin \omega t,$$
$$\dot{y} = b\, x - x^2\, y, \qquad (2)$$

Where, a and b are constants with $a, b > 0$, x and y represent the dimensionless concentrations of two reactants. f is the unmodulated carrier amplitude, $2g$ is the degree of modulation, ω and Ω are the two frequencies of the AM force. Recently, the AM force has been applied to certain nonlinear systems [20-23] to investigate certain nonlinear phenomena such as horseshoe chaos, vibrational resonance etc. The main objective of this article is to numerically study the occurrence of hysteresis, vibrational resonance and chaos in Brusselator model (Eq.2) under the excitation of amplitude modulated (AM) force.

Equilibrium point and its stability analysis

Equilibrium point

The equilibrium point is obtained by substituting $\dot{x} = 0$, $\dot{y} = 0$ and without any external force

$$a - x = 0, \qquad b = x\, y \qquad (3)$$

Thus, there is only one equilibrium point, namely

$$(x^*,\ y^*) = (a,\ b/a) \qquad (4)$$

Stability of Equilibrium Point

The stability determining eigenvalues are obtained from

$$\det (M - \lambda I) = \begin{vmatrix} b - 1 - \lambda & a^2 \\ -b & -a^2 - \lambda \end{vmatrix} = 0 \qquad (5)$$

Expanding the determinant, we obtain

$$\lambda^2 + \lambda\ (a^2 - b + 1) + a^2 = 0 \qquad (6)$$

Thus the eigenvalues are,

$$\lambda_{1,\,2} = \frac{1}{2}[-(a^2 - b + 1) \pm \sqrt{((a^2 - b + 1)^2 - (2a)^2}\,] \qquad (7)$$

If $b > (a^2 + 1)$ then the eigenvalues of the fixed points λ_1 and λ_2 are complex conjugates with real part greater than zero and hence the equilibrium point is unstable. If $b < (a^2 + 1)$, the corresponding eigenvalues λ_1 and λ_2 are complex conjugates with real part less than zero and hence the equilibrium point is stable. If $b = (a^2 + 1)$, the eigenvalues λ_1 and λ_2 of the fixed points are purely imaginary that is, $\lambda_{1,2} = \pm\, ia$ and hence the equilibrium point is center or elliptic.

Effect of AM Force in System-2 with Ω >> ω

In this section, we analyze the effect of AM force in Brusselator system-2 with the frequencies of the force Ω >> ω.

Vibrational Resonance

In a nonlinear dynamical system driven by a biharmonic force consisting of a low and high–frequencies ω and Ω with Ω >> ω, when the amplitude *g* of the high frequency force is varied, the response amplitude at the low frequency ω exhibits a resonance. This high-frequency force induced resonance is called *Vibrational Resonance(VR)* [24,25]. The analysis of VR has received a considerable interest in recent years because of its wide variety of applications in engineering and science. The occurrence of VR has been studied in monostable [26], bistable [24,25], multistable [27], maps [28] and exitable and specially extended systems [29].

Hysteresis

In the present paper, the parameters of the system (2) are chosen as $a = 0.4$, $b = 1.2$, $f = 0.1$, $\omega = 0.81$ and $\Omega = 50\omega$. First we analyze the occurrence of hysteresis which is the necessary condition for the occurrence of VR. A bifurcation diagram plotted by varying g in the forward direction as well as in the reverse direction is shown in **Figure 1**. Coexistence of several attractors and hysteresis are observed when *g* is varied. Figure 1(a) is obtained by varying the amplitude *g* from a small value in the forward direction. Figure 1(b) is obtained by varying *g* in the reverse direction from the value 1. Different paths are followed in the Figures 1(a) and 1(b). That is the system exhibits hysteresis when the control parameter *g* is varied smoothly from a small to a larger and then back to a small value.

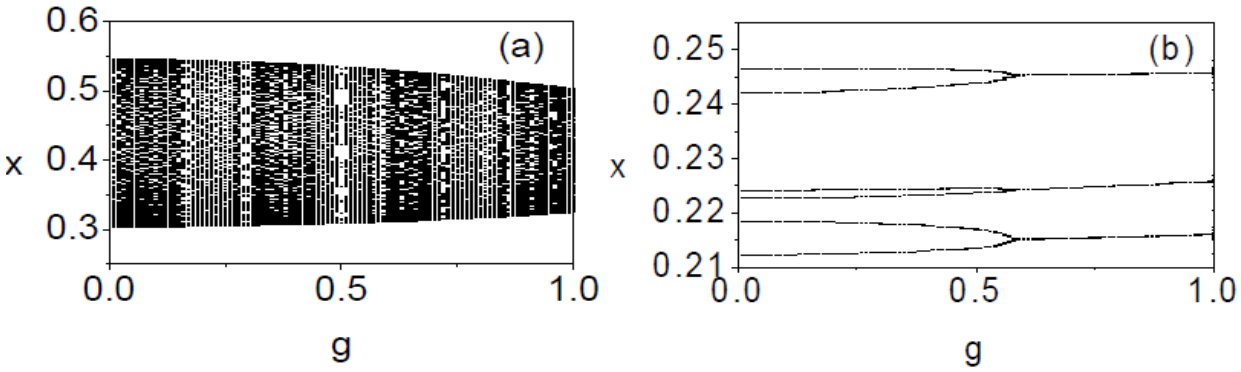

Figure 1 Bifurcation diagrams (a) *g* is varied in the forward direction from 0. (b) *g* is varied in the reverse direction from 1. The parameters are fixed as $a = 0.4$, $b = 1.2$, $f = 0.1$, $\omega = 0.81$ and $\Omega = 50\omega$.

Response Amplitude (Q)

In addition to the hysteresis, the system-2 exhibits also the phenomenon of VR when g is varied. To quantify the occurrence of VR, we use the response amplitude *Q* of the system-2 at the signal frequency (ω). The system-2 is numerically integrated using fourth-order Runge-Kutta method with time step size $(2\pi/\omega) / 1000$. The first 10^3 drive cycles are left as transient and the values of *x(t)* corresponding to the next 500 drive cycles are used to compute the response amplitude. From the numerical solution of *x(t)*, the response amplitude *Q* is computed through $Q = \sqrt{Q_S^2 + Q_C^2}\,/\,f$, where

$$Q_S = \frac{2}{nT}\int_0^{nT} x(t)\sin\omega t\,dt,$$

$$Q_C = \frac{2}{nT}\int_0^{nT} x(t)\cos\omega t\,dt \qquad (8)$$

where $T = (2\pi/\omega)$ is the period of the response and *n* is taken as 500.

We numerically calculate Q with a low frequency force only, a high-frequency force only and with both forces. In the case of $f = 0$, the response amplitude Q is measured as $Q = \sqrt{Q_S^2 + Q_C^2}$, Q_S and Q_C measure the coefficients of the Fourier sine and cosine components respectively of the output signal at the frequency $2\pi/T$. Q measures the amplitude of the response at the frequency $2\pi/T$. When the system-2 is driven by only one force (ie. $f = 0$ or $g = 0$) the variation of numerically calculated Q with f and g is shown in **Figure 2**. In Figure 2(a) when f is varied and $g = 0$, the response amplitude Q increases to a maximum and then decreases resulting in the formation of single peak at $f = 0.06537$ with $Q_{max} = 1.9033$. But in Figure 2(b) multiple peaks are observed when g is varied with $f = 0$.

Figure 3 shows a completely different result when both forces are switched on. Figures 3(a) and 3(b) illustrate the variation of numerically computed Q with g for different values of f and ω. When g is varied, the response amplitude Q increases to a maximum and then decreases resulting in the formation of peak and hence this phenomenon is termed as VR as it is due to the presence of high-frequency external periodic force. The maximum value of the peak is detected when the values of f and ω are 0.02 and 0.41, respectively.Thus it is clear that the positions of the extrema of Q depend on f and ω. In Figure 3(a), for $f = 0.02$, 0.05 and 0.1, as g increases from zero the value of Q increases, it reaches a maximum and then decreases. But for $f = 0.15$ as g increases, Q decreases and no resonance is observed. In Figure 3(b) for ω = 0.20, 0.41, 0.61 and 0.81, the response amplitude Q is found to be maximum at g =0.691, 0.945, 2.638, 2.087 respectively.

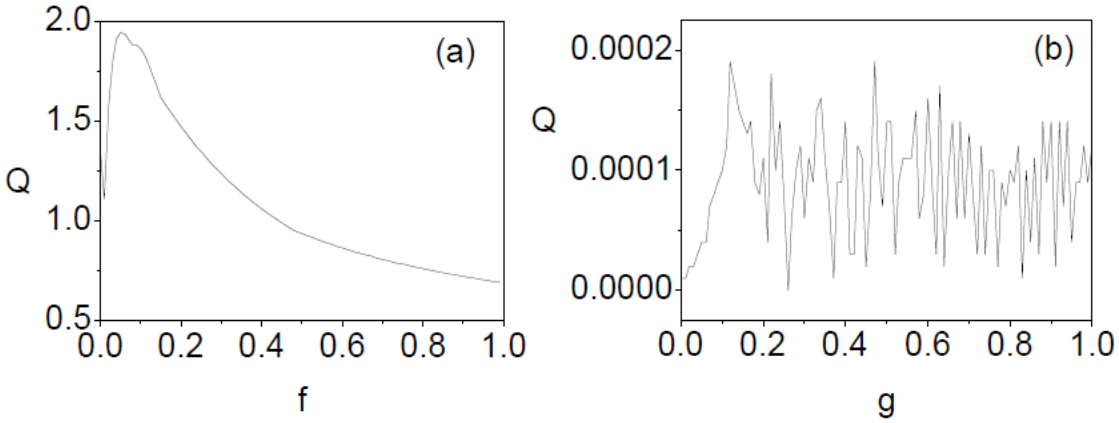

Figure 2 (a) Response amplitude Q versus f for $g = 0$. (b) Q versus g for $f = 0$. The values of the other parameters are $a = 0.4$, $b = 1.2$, ω = 0.81 and Ω = 50ω.

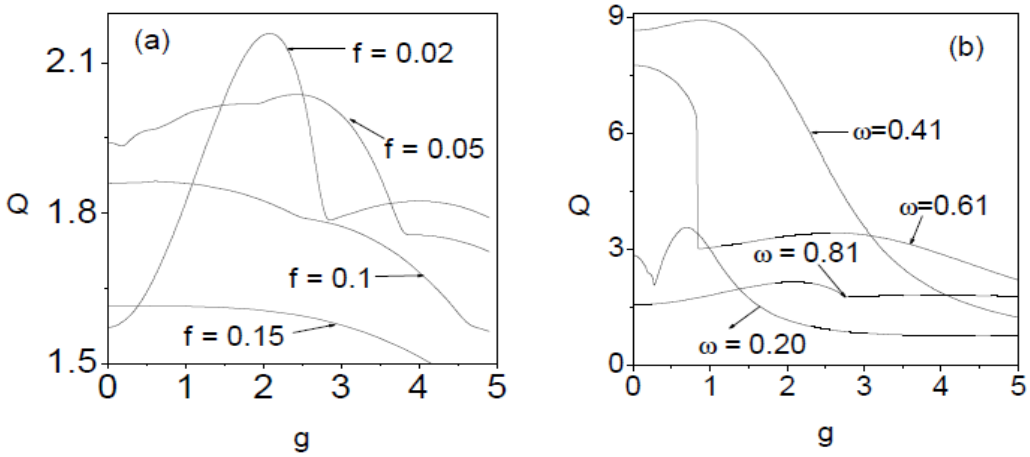

Figure 3 (a) Response amplitude Q versus g for four values of f. (b) Q versus g for four values of ω. The values of the other parameters are as $a = 0.4$, $b = 1.2$, $f = 0.1$, ω = 0.81 and Ω = 50 ω.

Figures 4 and **5** show the phase portraits and trajectory plots for a few values of g in the interval [0, 5] for f = 0.02, ω = 0.81 and Ω = 50 ω. In all the regions the motion is periodic with the period $T = 2\pi / \omega$. By increasing the amplitude g of the high-frequency force, the system-2 is found to exhibit numerically a sequence of bifurcations. Starting from equilibrium, the solution bifurcates through a Hopf bifurcation to a limit cycle and then by period-doubling sequences. These are illustrated in Figures 4 and 5.

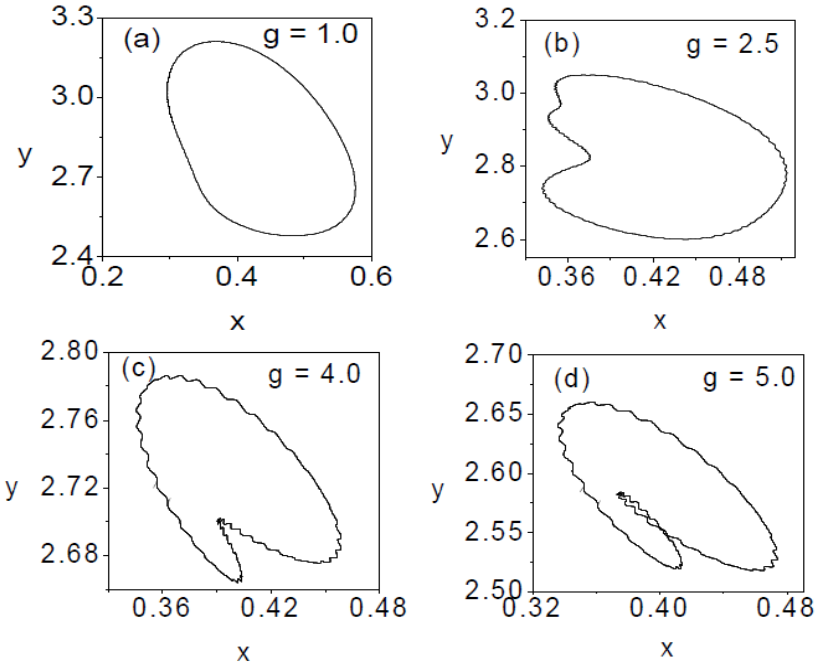

Figure 4 Phase portraits for different values of high-frequency amplitude g. The values of the other parameters are as a = 0.4, b = 1.2, f = 0.02, ω = 0.81 and Ω = 50ω

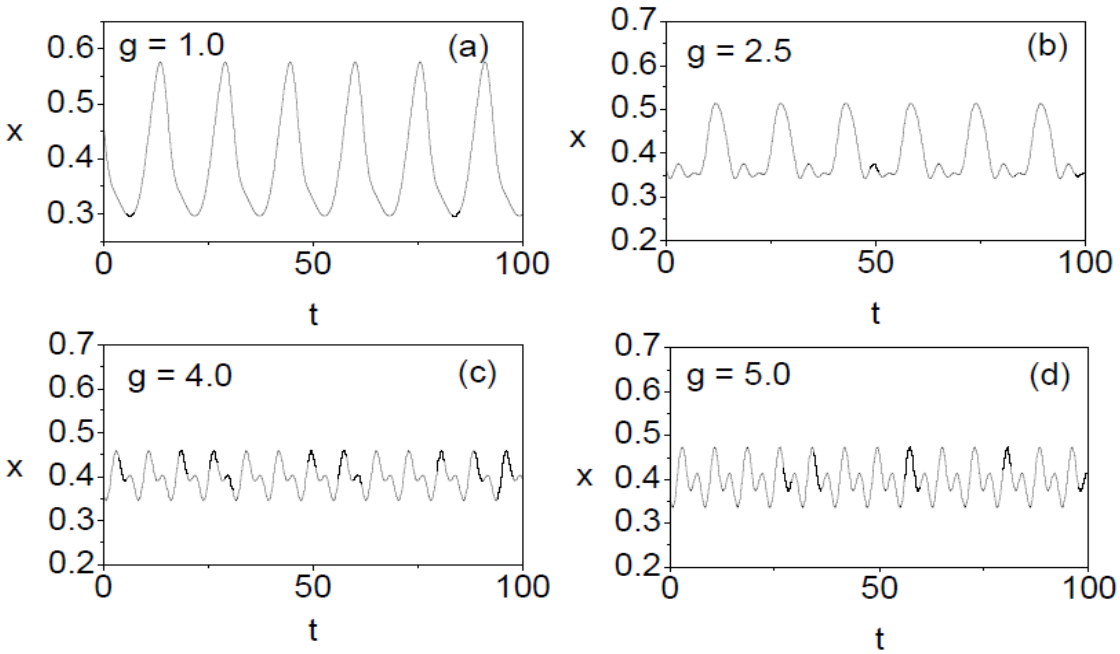

Figure 5 Trajectory plots for different values of high-frequency amplitude g. The values of the other parameters are as a = 0.4, b = 1.2, f = 0.02, ω = 0.81 and Ω = 50ω.

Effect of AM Force in System-2 With ω = Ω

In the previous section, we have shown the occurrence of hysteresis and vibrational resonance in system-2 driven by AM force with Ω >> ω. In this section, we show the occurrence of coexistence of several attractors, different routes to chaos and suppression of chaos in the presence of AM force with $\omega = \Omega$.

We fix the values of the parameters as $a = 0.4$, $b = 1.2$ and $\omega = \Omega = 0.81$. For a range of f and g the system-2 has coexistence of several attractors. When the control parameter f or g is varied, the system-2 underwent quaiperiodic, period-doubling bifurcations leading to chaotic motion at some critical values. **Figure 6**(a) shows the bifurcation diagram where g is set to zero while f is varied. As f is increased from zero, a quasiperiodic orbit occurs which persist up to $f = 0.00955$ and then it loses its stability giving birth to a period-doubling orbits. These orbits accumulate at $f = f_c = 0.04578$. At this critical value of f onset of chaotic motion occurs. When the control parameter f is increased from f_c, one finds that the chaotic orbits persist for a range of f values followed by reverse period doubling bifurcation. At $f = 0.481$, the reverse period doubling bifurcation disappears and the long time motions settle to a periodic behavior. It shows that quasiperiodic, periodic, chaotic and reverse period–doubling motions coexist for the range $f \in [0, 0.5]$. In **Table 1**, we give a succinct account of the different types of attractors admitted by the system-2 driven by an AM force with $g = 0$ and $\omega = \Omega$.

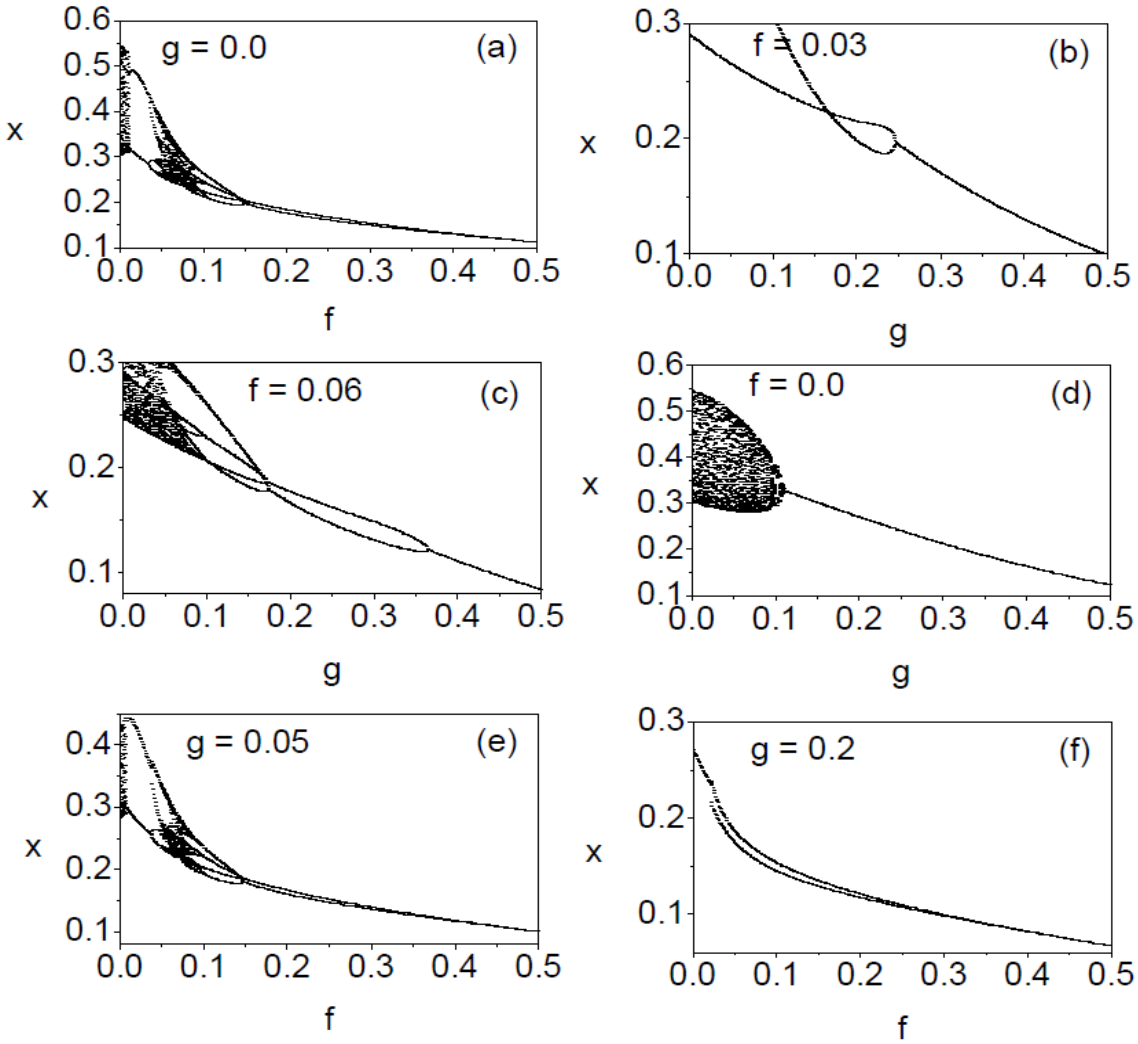

Figure 6 Bifurcation structures for $a = 0.4$, $b = 1.2$, $\omega = \Omega = 0.81$

Table 1 Summary of bifurcation phenomena of system-2 with $a = 0.4$, $b = 1.2$, $\omega = \Omega = 0.81$ and $g = 0$

Value of f	Nature of solution
$0 < f < 0.00955$	Quasiperiodic orbit
$0.00955 < f < 0.04578$	Period doubling orbit
$0.04578 < f < 0.09514$	Chaos
$0.09514 < f < 0.481$	Reverse period doubling orbit
$0.481 < f < 1.0$	Period-T orbit

We show the effect of the control parameter g by fixing the values of f in a regular region and then in a chaotic region. For $f = 0.3$ and $g = 0$ the motion of the system is periodic with period–2T. Figure 6(b) is the bifurcation diagram obtained by varying g from 0 to 0.5. As g is increased from zero the reverse period-2T orbit persists up to $g = 0.245$ after that the long time motion settles to a period-T orbit. Figure 6(c) corresponds to $f = 0.06$ (chaotic motion when $g = 0$). When the control parameter g is smoothly varied, the system-2 starts with chaotic motion followed by reverse period doubling bifurcation. Periodic behavior is observed for the range $0.362 < g < 0.5$. That is, the parameter g can be used to suppress chaotic motion by choosing its value in the above interval.

The bifurcation diagram corresponding to $f = 0$ and $g \in [0, 0.5]$ is shown in Figure 6(d). As g is increased from zero, a stable quasiperiodic orbits occurs, which persists up to $g = 0.1$. At $g = 0.1$ the quasiperiodic motion suddenly disappears and the long term motion settles to periodic behavior. The influence of the control parameter f on the dynamics for the two fixed values of g, namely $g = 0.05$ (quasiperiodic region) and 0.2 (periodic region) is also studied. The effect of f can be clearly seen in the bifurcation diagrams Figures 6(e) and 6(f). Here again suppression of chaos is found for certain range of values of the control parameter f. An example of quasiperiodic, periodic and chaotic attractors is shown in **Figures 7**(a), 7(c) and 7(e) and the corresponding Poincare maps is shown in Figures 7 (b), 7(d) and 7(f).

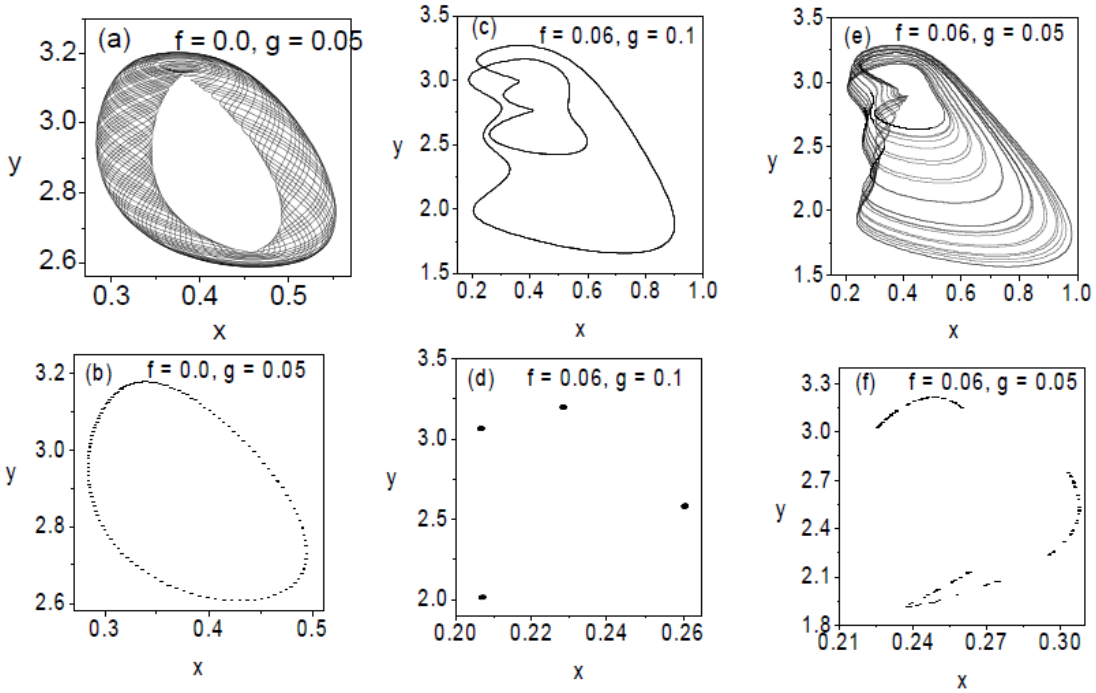

Figure 7 (a-b) Quasiperiodic orbit for $f = 0$, $g = 0.05$ (c-d) Period-4T orbit for $f = 0.06$, $g = 0.1$ (e-f) Chaotic orbit for $f = 0.06$, $g = 0.05$. The parameters are fixed as $a = 0.4$, $b = 1.2$, $\omega = \Omega = 0.81$.

Next, we consider the system-2 subjected to the AM force with incommensurate frequencies. In our numerical study, we fixed $\omega = 0.81$ and $\Omega = (\sqrt{5} - 1) / 2$, the reciprocal of the golden mean. The external force is now quasiperiodic. **Figure 8** presents bifurcation diagrams and the corresponding maximal Lyapunov exponents (λ) of two sets of values of the parameter f and g. For the calculation of all Lyapunov exponents we used the algorithm of Wolf et al. [30]. The maximal Lyapunov exponent is found to be negative for periodic behaviour, positive for chaotic dynamics and ≈ 0 at

bifurcation points. In Figures 8(a) and 8(b) *g* is kept at 0.1 while *f* is varied, λ is completely negative in all the range of values of *f*. Quasiperiodic motion is completely observed and no periodic and chaotic motions are observed. An example of quasiperiodic attractors are shown in **Figure 9** for different values *f* = 0.1, 0.3, 0.7 with *g* = 0.1. In Figures 8(c) and 8(d), *f* is kept 0.1 while *g* is varied. λ is positive only in a small range of *g* values. Quasiperiodic motion is widely observed. Examples of chaotic and quasi- periodic attractors are shown in **Figure 10** for different values of g.

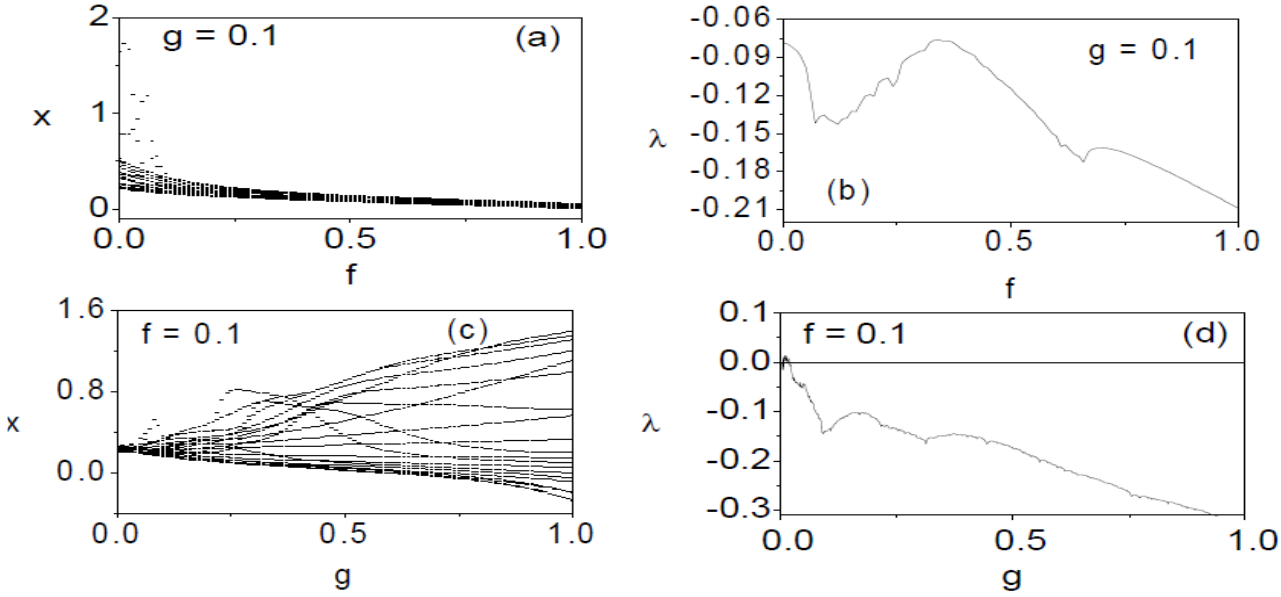

Figure 8 Bifurcation structures and the corresponding maximal Lyapunov exponent diagrams for *a* = 0.4, *b* = 1.2, ω = 0.81 and Ω = ($\sqrt{5}$ -1) / 2

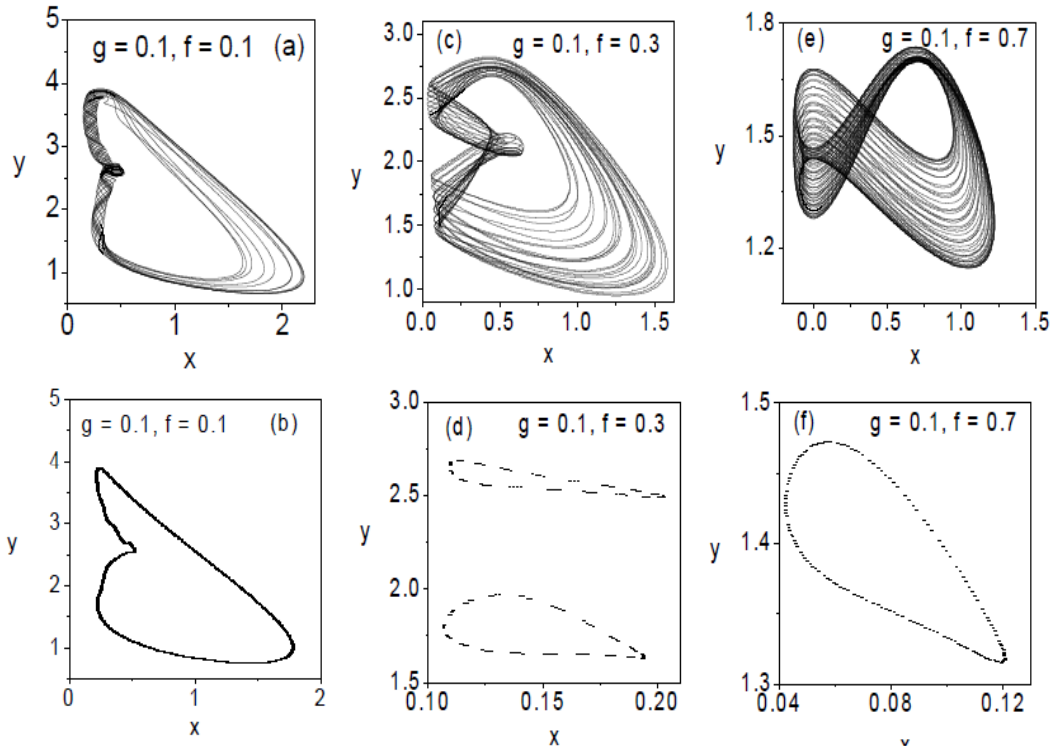

Figure 9 Quasiperiodic orbits for different values of *f*. The other parameters are *a* = 0.4, *b* = 1.2, *g* = 0.1, ω = 0.81 and Ω = ($\sqrt{5}$ -1) / 2.

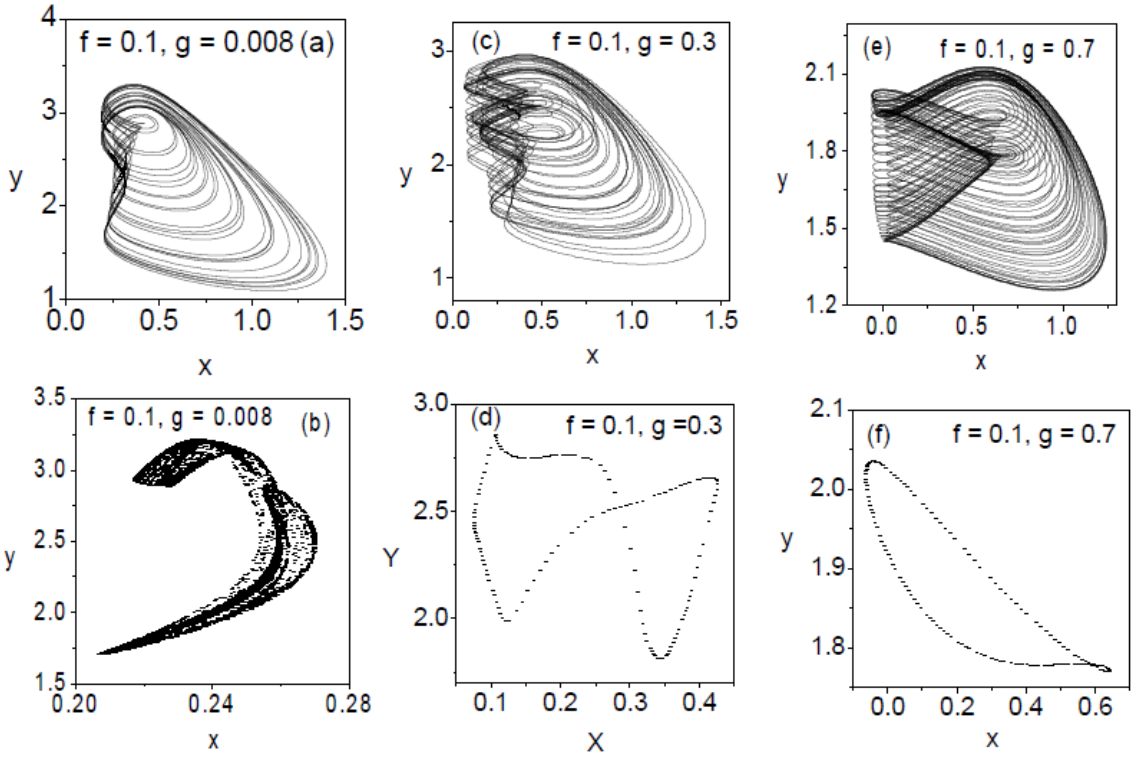

Figure 10 Phase portraits and Poincare maps for (a-b) chaotic orbit for g = 0.008 (c-d) quasiperiodic orbits for g = 0.3 and (e-f) for g = 0.7. The other parameters are a = 0.4, b = 1.2, f = 0.1, ω = 0.81 and Ω = ($\sqrt{5}$ -1) / 2

Summary and Conclusion

In the present paper we considered the Brusselator chemical system subjected to an AM force. We numerically studied the effect of external force with Ω >> ω. We have observed the occurrence of hysteresis and vibrational resonance in system-2 when it is subjected to an AM force one with the frequency larger than the other (Ω >> ω). Changing the amplitude of the high frequency component improves signal processing of the low frequency component in a resonant way. From numerical analysis, we were able to observe multiple resonant peaks for different values of the control parameters, say, the amplitude, frequency of low frequency signal (f and ω) and the amplitude of the high-frequency vibrational signal (g).

Next we numerically studied the dynamics of the system-2 for Ω = ω. Coexistence of several attractors and bifurcations of them are found. The AM force which we considered in the present work has four parameters such as f, g, Ω and ω. As shown in Figure 6 the presence of additional parameters can be used to control and anti-control of chaos. The additional features of the system in terms of ghost vibrational resonance, parametric resonance, coherent resonance etc deserve for further study.

References

[1] R.J. Field, M. Burger, *Oscillations and Travelling Waves in Chemical Systems*, Wiley–Interscience, New York, 1985.
[2] S.K. Scott, *Chemical Chaos*, Oxford University Press, Oxford, 1991.
[3] P. Gray, S.K. Scott, *Chemical Oscillations, Instabilities: Nonlinear Chemical Kinetics*, Oxford University Press, Oxford, 1990.
[4] J. Wang, H. Sun, S.K. Scott, K. Showalter, *Phys. Chem. Chem. Phys*., 2003, 5, 5444.
[5] I.R. Epstein, K. Showalter, *J. Phys. Chem*., 1996, 100, 13132.
[6] J. Shi, *Front. Math*. China 2009, 4, 407.
[7] J. Tyson, *J. Chem. Phys*., 1973, 58, 3919.
[8] R. Lefever, G. Nicolis, *J. Theor. Biol*., 1971, 30, 267.

[9] E. Ott, *Chaos in Dynamical Systems*, Cambridge University Press, Oxford, 1993.
[10] R. deBarros Faria, I. Lengyel, I.R. Epstein, K. Kustin, *J. Phys. Chem*. 1993, 97, 1164.
[11] L. Prigogine, R. Lefever, *J. Chem. Phys.*, 1968, 48, 1695.
[12] T. Ma, S. Wang, *J. of Math. Phys*., 2011, 52, 033501.
[13] M. Sun, T. Tan, L. Chen, *J. Math. Chem*., 2008, 44, 637.
[14] J.C. Tzou, B.J. Matkowsky, V.A. Volpert, *Appl. Math. Lett*., 2009, 22, 1432.
[15] T. Kai, K.Tomita, Prog. *Theor. Phys*., 1979, 61, 54.
[16] K. Tomita, T. Kai, *J. Stat. Phys*., 1979, 21, 65.
[17] B.L. Hao, S.Y. Zhang, *J. Stat. Phys*., 1982, 28, 769.
[18] I. Bashkirtseva, L. Ryashk, *Chaos, Soliton and Fractals*, 2005, 26, 1437.
[19] Ali Sanayei, *Proceedings of the World Congress on Engineering* (WCE), Vol. III, June 30-July 2, 2010, London, UK.
[20] V.M. Gandhimathi, S. Rajasekar, *Phys. Scr*., 2007, 76, 693.
[21] Y.C. Lai, Z. Liu, A. Nachman, L. Zhu, Int. J. Bifur. *Chaos Appl. Sci. Eng*. 2004, 14, 3719.
[22] V. Ravichandran, V. Chinnathambi, S. Rajasekar, *Physica A* 2007, 376, 223.
[23] J.H. Yang, X.B. Liu, *Phys. Scr*., 2010, 82, 025006.
[24] P.S. Landa, P.V.E. McClintock, *J. Phys A:Math.Gen*., 2000, 33, 1433.
[25] I.I. Blekhman, P.S. Landa, Int. *J. Nonlinear Mechanics*, 2004, 39, 421.
[26] S. Jeyakumari, V. Chinnathambi, S. Rajasekar, M.A.F. Sanjuan, *Phys. Rev. E*, 2009, 80, 041608.
[27] S. Rajasekar, K. Abirami, M.A.F. Sanjuan, *Chaos*, 2011, 21, 033106.
[28] S. Rajasekar, J. Used, A. Wagemakers, M.A.F. Sanjuan, *Commun. Nonlinear Sci. Number. Simulat*., 2012, 17, 3435.
[29] E. Ullner, A. Zaikin, J. Garcia-Ojalvo, R. Bascones, J. Kurths, *Phys. Lett. A*, 2003, 312, 348.
[30] A. Wolf, J.B. Swift, H.L. Swinny, J.A.Vastano, *Physica D*, 1985,16, 285.

Publication History
Received 10th July 2015
Revised 20th July 2015
Accepted 13th Aug 2015
Online 30th Aug 2015